LUNAR ROCK MAGNETISM

T. NAGATA

Geophysics Research Laboratory, University of Tokyo, Tokyo, Japan

and

R. M. FISHER and F. C. SCHWERER

U.S. Steel Corporation Research Center, Monroeville, Penns., U.S.A.

Abstract. The relationship between the magnetization and temperature in a high constant magnetic field for a temperature range between 5 K and 1100 K was examined for Apollo 11, 12 and 14 lunar materials. The average value of Curie point temperature is (768.2 ± 3.5)°C for the lunar igneous rocks and (762.5 ± 3.4)°C for the lunar fines and breccias. A tentative conclusion about the ferromagnetic substance in the lunar materials would be that Fe is absolutely dominant with a slight association of Ni and Co, and probably Si also, in the lunar native irons.

The antiferromagnetic phase of ilmenite and the paramagnetic phase of pyroxenes are considerably abundant in all lunar materials. However, a discrepancy of observed magnetization from a simulated value based on known magnetic elements for the temperature range between 10 and 40 K suggests that pyroxene phase represented by $(M_x\mathrm{Fe}_{1-x})\,\mathrm{SiO}_3$ (where $M = \mathrm{Ca}^{2+}$, Mg^{2+}, etc and $0 \leq x \leq \frac{1}{4}$) also may behave antiferromagnetically.

Magnetic hysteresis curves are obtained at 5 K and 300 K, and the viscous magnetic properties also are examined for a number of lunar materials. The superparamagnetically viscous magnetization has been experimentally proven as due to fine grains of metallic iron less than 200 Å in mean diameter. The viscous magnetization is dominant in the lunar fines and breccias which is classified into Type II, while it is much smaller than the stable magnetic component in lunar igneous rocks (Type I). The superparamagnetically fine particles of metallic iron are mostly blocked at 5 K in temperature; thus coercive force (H_c) and saturation remanent magnetization (I_R) become much large at 5 K as compared with the corresponding values at 300 K.

Strongly impact-metamorphosed parts of lunar breccias have an extremely stable NRM which could be attributed to TRM. NRM of the lunar igneous rocks and majority of breccias (or clastic rocks) are intermediately stable, but their stability is considerably higher than that of IRM of the same intensity. This result may imply that some mechanism which causes an appreciable magnitude of NRM and the higher stability, such as the shock effect, may take place on the lunar surface in addition to TRM mechanism for special cases.

A particular igneous rock (Sample 14053) is found to have an unusually strong magnetism owing to a high content of metallic iron (about 1 weight percent), and its NRM amounts to 2×10^{-3} emu/g. The abundance of such highly magnetic rocks is not known as yet but it seems that the observed magnetic anomalies on the lunar surface could be related to such highly magnetized rock masses.

1. Introduction

From the results of various studies of the magnetic properties of Apollo 11 and 12 lunar materials, general magnetic characteristics of the lunar materials, particularly in comparison with those of terrestrial rocks, seem to have been at least qualitatively understood. The experimental results obtained independently by different investigators are in good agreement with one another in regard to a number of characteristic features of the lunar rocks magnetism, although few numbers of magnetically particular samples also have been reported.

Communication presented at the Conference on Lunar Geophysics, held between October 18–21, 1971, at the Lunar Science Institute in Houston, Texas, U.S.A.

From observed data of the intrinsic magnetic properties of the lunar materials such as the saturation magnetization (I_s) and Curie point temperature (Θ_c), it has been concluded that the absolute majority of ferromagnetic minerals in the lunar materials are native irons. This is a striking contrast to the case of terrestrial rocks, in which the absolute majority of magnetic minerals are titanoferous magnetites, $x\mathrm{Fe_2TiO_4}(1-x)\,\mathrm{Fe_3O_4}$, a solid solution series between magnetite and ulvöspinel, which are, strictly speaking, ferrimagnetic substances.

The intrinsic magnetic properties of the lunar igneous rocks have been identified to those of nearly pure metallic irons, and the abundance of metallic iron in them is estimated to be less than only 0.1 weight percent in most cases. The magnetic properties of the lunar breccias (the lunar fragmented rocks) and fines have shown that their ferromagnetism is attributable to either almost pure irons or iron-nickel alloys. The abundance of the ferromagnetic component in these samples has been estimated to be much higher than that in the igneous rocks, amounting to $0.5\sim1.0$ weight percent. These magnetic results are in good agreement with the results of petrographical and mineralogical observations of the metallic components in the lunar materials: that is, in igneous rocks, the metallic iron occurs within the troilite (FeS) blebs, usually rounded inclusions but occasionally showing cubic crystal forms, and this metal is essentially pure iron with very little nickel (0.1% or less); on the other hand, the breccias and the lunar soils contain a nickelferous iron usually as irregular fragments up to a few millimeter across but sometimes as spherical or lensoid droplets (e.g. Mason and Melson, 1970; Levinson and Taylor, 1971).

It seems thus that both magnetic and mineralogical studies on the lunar materials have led to a conclusion that the metallic iron is present in the lunar materials in two distinct forms: one inherent to the lunar igneous rocks and one introduced by impacting meteorites. It seems thus that a considerable amount of metallic irons of the meteoritic origin is included in the lunar fines and breccias. This conclusion may be supported also by geochemical data of the lunar materials. The bulk abundance of Ni is generally less than 30 ppm in the lunar igneous rocks, while it amounts to as high as $150\sim300$ ppm in the lunar fines and breccias. These geochemical data may suggest that metallic irons including an appreciable amount ($5\sim10\%$) of Ni have been introduced into the lunar fines and breccias, resulting in an increase of metallic iron abundance by about one order of magnitude.

The structure-sensitive magnetic properties such as the saturation remanent magnetization (I_R), the coercive force (H_c), the remanence coercive force (H_{RC}) and the initial reversible magnetic susceptibility (χ_0) of the lunar materials have indicated, on the other hand, that the grain size of these metallic irons ranges from a very fine grain of the superparamagnetic character at room temperature to a magnetically stable multidomain grain. In general, the very fine grains of metallic irons having the superparamagnetic or pseudosuperparamagnetic character at room temperature occupy a considerable portion of the ferromagnetics in the lunar fines and breccias. Hence, the viscous magnetization becomes dominant in the lunar fines and breccias in presence of even a weak magnetic field, such as the geomagnetic field. In the case

of terrestrial rocks, the superparamagnetic (or viscous) magnetization occupies only a little portion of their whole magnetization in most cases, an appreciable viscous magnetization taking place only in exceptionally special cases. It may be considered therefore that the general presence of viscous magnetization is one of characteristic features of the lunar rock magnetism. The natural remanent magnetization (NRM) of the lunar igneous rocks and breccias may be one of the main subjects in the lunar rock magnetism, since its paleomagnetic interpretation is directly related to the studies on the evolution of the Moon. As the acquisition mechanism of the observed NRM of the lunar rocks, several possible processes which have been found in terrestrial rocks, such as the isothermal remanent magnetization (IRM), the thermoremanent magnetization (TRM), the chemical remanent magnetization (CRM), the pressure remanent magnetization (PRM) and the shock remanent magnetization (SRM) have been presumed individually or combinedly by various workers.

We might have to examine, however, whether or not the physical basis of the lunar rock magnetism can be exactly the same as that of terrestrial rock magnetism with respect of its every detail, because, in the lunar rocks, the bearers of NRM are metallic iron grains and a considerable portion of the metallic irons is in form of the superparamagnetically fine grain. We have now some variety of the lunar rock samples returned by Apollo 11, 12 and 14 Missions. The main purpose of this paper is to describe the magnetic properties of the lunar materials as systematically as possible at the present stage based mostly upon the authors' own results of measurement.

An additional remark might have to be made in regard to the paramagnetic and antiferromagnetic components in the lunar materials. Very few studies have been made so far on the paramagnetic and antiferromagnetic components in terrestrial rocks. This might be due to a fact that these components can be ignored in examining the ferrimagnetism of terrestrial rocks, though they ought to be present in terrestrial rocks also. On the other hand, the paramagnetic and antiferromagnetic magnetizations are not negligibly small compared with the ferromagnetic one in the lunar materials, particularly in the lunar igneous rocks. This is the reason why the paramagnetism and antiferromagnetism of the lunar materials also are described in this paper.

2. Ferromagnetic Substances in the Lunar Materials

The intrinsic and structure-sensitive magnetic parameters of Apollo 11, 12 and 14 materials were examined by (1) measuring the magnetization curve for the magnetic field range from -16 to 16 kilo-Oe at room temperature (about 300 K) with a special additional measurement of the remanence coercive force (H_{RC}), (2) measuring the magnetization versus temperature curve in the heating and cooling processes in the temperature range from 20 °C to 850 °C in vacuum of less than 10^{-5} T of air pressure in a reasonably strong magnetic field of about 5.5 kilo-Oe in intensity, (3) measuring the magnetization versus temperature curve in the temperature range from 5 K to 300 K in a magnetic field stronger than 3 kilo-Oe. Figures 1 and 2 show examples of the magnetization curves of Apollo 14 igneous rock, No. 14053–48,

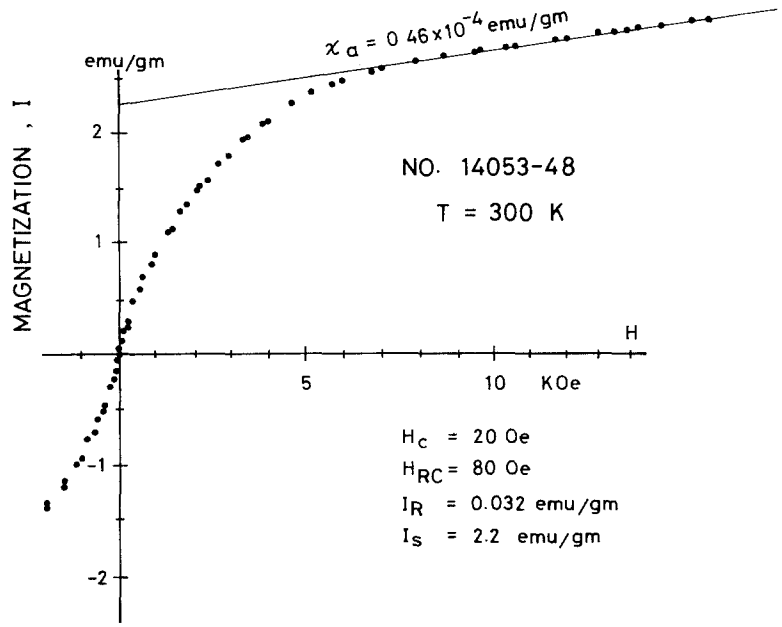

Fig. 1. Magnetic hysteresis curve of Sample 14053–48 measured at 300 K.

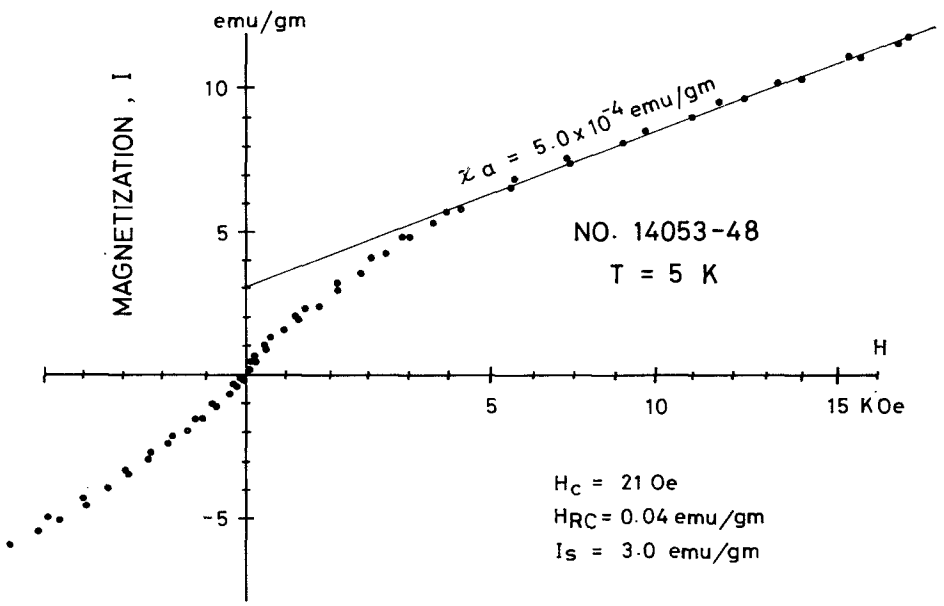

Fig. 2. Magnetic hysteresis curve of Sample 14053–48 measured at 5 K. (H_{RC} be read I_R).

observed at 300 K and 5 K respectively by a vibration magnetometer. The intensity of magnetization, $I(H)$, observed at a magnetic field H is assumed to be a sum of a ferromagnetization which is subjected to the magnetic hysteresis curve, $I_F(H)$, and a paramagnetization $\chi_a H$, where the paramagnetic susceptibility (χ_a) includes the susceptibility of antiferromagnetic component: namely,

$$I(H) = I_F(H) + \chi_a H . \tag{1}$$

The linear relationship between $I(H)$ and H for large values of H where the ferromagnetization is practically saturated represents the paramagnetic component $\chi_a H$. Subtracting $\chi_a H$ form $I(H)$, the ferromagnetic hysteresis curve $I_F(H)$ is obtained as a function of H. The saturation magnetization (I_s), the saturation remanent magnetization (I_R) and the coercive force (H_c) of the ferromagnetic component as well as χ_a thus evaluated for the igneous rocks, fines, and clastic rocks or breccias of the lunar materials are summarized in Tables I, II, and III respectively. In Figures 1 and 2, details of the $I(H) \sim H$ relation are not well illustrated because of a large scale of coordinates, but I_R and H_c could practically be determined with observational errors of $\pm 5\%$.

TABLE I

Basic magnetic properties of lunar igneous rocks

Magnetic parameters	10024-22	12053–47	14053–48	Unit
χ_0	2.6	2.6	2.24	$\times 10^{-4}$ emu/g
χ_a	3.4	3.4	4.6	$\times 10^{-5}$ emu/g
I_s	0.155	0.195	2.2	emu/g
I_R	0.15	0.08	4.0	$\times 10^{-2}$ emu/g
H_c	45	8	20	Oe
H_{RC}	160	76	80	Oe
Θ_C	765(± 5)	760(± 8)	765(± 5)	°C

χ_0 : Initial reversible magnetic susceptibility at 300 K.
χ_a : Paramagnetic susceptibility at 300 K.
I_s : Saturation magnetization at 300 K.
I_R : Saturation remanent magnetization at 300 K.
H_c : Coercive force at 300 K.
H_{RC} : Remanence coercive force at 300 K.
Θ_C : Curie point temperature.

TABLE II

Basic magnetic properties of lunar fines

Magnetic parameters	10084–89	12070–102	14259–69	Unit
χ_0	8.3	7.2	10.0	$\times 10^{-3}$ emu/g
χ_a	3.5	2.5	2.5	$\times 10^{-5}$ emu/g
I_s	1.17	1.28	1.50	emu/g
I_R	8.4	6.2	6.0	$\times 10^{-2}$ emu/g
H_c	36	22	19	Oe
H_{RC}	460	450	300	Oe
Θ_c	775(± 10)	770(± 8)	750(± 5)	°C

TABLE III

Basic magnetic properties of lunar breccias and clastic rocks

Magnetic parameter	10021–32	10048–55	10085–13	14047–47	14301–65	14303–35	14311–45	Unit
χ_0	8.6	9.6	4.3	8.0	0.93	0.69	0.46	$\times 10^{-3}$ emu/g
χ_a	–	4.3	4.4	2.4	2.1	2.4	2.3	$\times 10^{-5}$ emu/g
I_s	0.74	1.8	0.44	1.40	0.69	1.27	0.74	emu/g
I_R	5.0	13.0	6.7	6.1	0.64	2.1	0.43	$\times 10^{-2}$ emu/g
H_c	19	50	125	26	27	27	19	Oe
H_{RC}	–	520	670	350	450	180	140	Oe
Θ_c	–	765 (±5)	–	760 (±5)	750* (±5)	735* (±5)	750* (±5)	°C

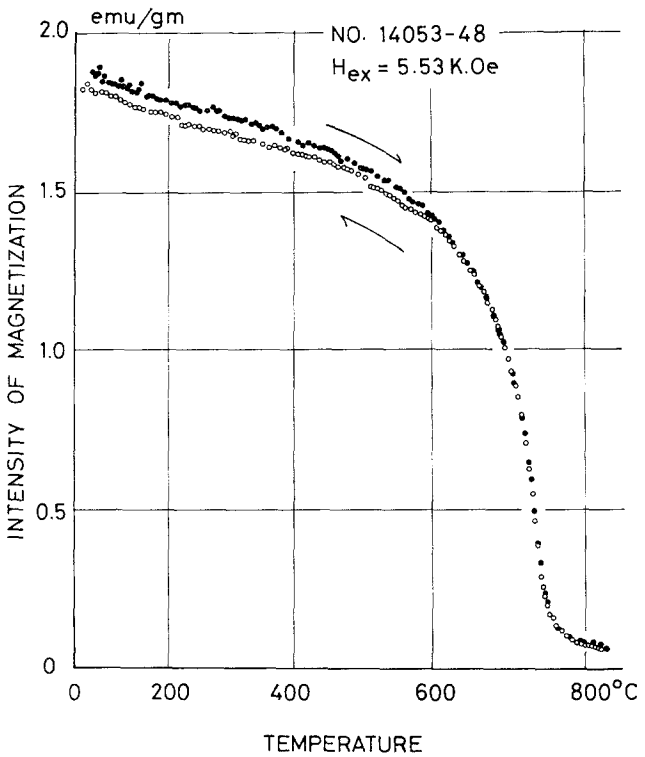

Fig. 3. Magnetization versus temperature curve measured in a magnetic field of 5.53 K Oe. Full circles- : heating process; hollow circles- : cooling process; Sample 14053–48.

Figures 3 and 4 show examples of the magnetization (I) versus temperature (T) curves for the range from 20 °C to 850 °C measured by a magnetic balance. In Figure 3, Curie temperature (Θ_c) of Sample No. 14053–48 is determined to be 765 ± 5 °C in both the heating and cooling curves which are in approximate agreement with each other.

In Figure 4(a), a systematic discrepancy of the cooling $I \sim T$ curve from the heating one of Sample No. 14303–35 is considerably large, but the magnitude of I in the cooling process has returned practically the same value as in the heating process at room temperature. Figure 4(b) illustrates the results of similar measurements of the same sample for the second run. The heating and cooling curves in the second run measurement are essentially identical to those in the first run measurement shown in Figure 4(a). This result indicates that the ferromagnetic component in this sample has an irreversible cycle with respect to temperature. A similar irreversible cycle of magnetization with respect to temperature has been observed in Samples No. 14301–65 and 14311–45 also. It must be noted here that the heating and cooling speed was always kept approximately at 200.° centigrade/hr in the *I-T* measurements. It is most likely that the irreversible cycle of magnetization with temperature is due to $\alpha \rightleftarrows \gamma$ transition of FeNi alloy (e.g. Bozorth, 1951), as already pointed out by Strangway *et al.* (1970) for an Apollo 11 lunar sample, No. 10084–90. Curie temperature is assigned to that in the heating curve in such a case.

Another example of the *I-T* measurement is shown in Figure 5, where the magnetization in the cooling curve is definitely smaller than that in the heating one, though Curie temperature is kept invariant. The *I-T* curves in the second run heating and cooling processes are practically in agreement with the first run cooling curve. It may be concluded therefore that a certain portion of the ferromagnetic component was lost by the first run heating procedure. This absolute irreversibility of magnetization with temperature by heating takes place in all lunar fines (10084–89, 12070–102 and 14259–69) and some clastic rocks (14047–47, 14301–65) and breccia (10048–55) which have been heated in vacuum of a little less than 10^{-5} T of air pressure. It seems likely that the loss of ferromagnetic component in the first heating process up to 850 °C is due to the oxidation of very fine free grains of metallic iron in the presence of low pressure oxygen. All observed values of Θ_c are listed in Table 1 through Table III.

Figure 6 shows example the magnetization (I) versus temperature (T) curves for the range from 5 K to 100 K, measured by a vibration magnetometer. The magnetization in this temperature range may be represented by a sum of ferromagnetic magnetization (I_F) which is almost independent of temperature, antiferromagnetic magnetization (I_A) and paramagnetic magnetization $\chi_a H$ where $\chi_a \backsim (1/T)$: namely,

$$I(H, T) = I_F(H) + I_A(H, T) + \chi_a(T)\, H\,. \tag{2}$$

It may be observed in Figure 6 that, in the lunar materials, the paramagnetic magnetization is markedly dominant in temperatures below 30 K and a superposition of an antiferromagnetic peak is noticeable at Néel temperature of ilmenite (57 K). Table I through Table III summarize the observed values of the intrinsic magnetic parameters (χ_a, I_s and Θ_c) and the structure-sensitive ones (χ_0, I_R, H_c and H_{RC}) of the lunar materials, where χ_0 denotes the initial reversible magnetic susceptibility measured by an alternating field magnetic susceptibility bridge of 1 kHz in frequency. It may be observed in these tables that Θ_c ranges from (735 ± 5) °C to (775 ± 10) °C, which are almost the same or a little lower than Curie point temperature of pure iron at 770 °C.

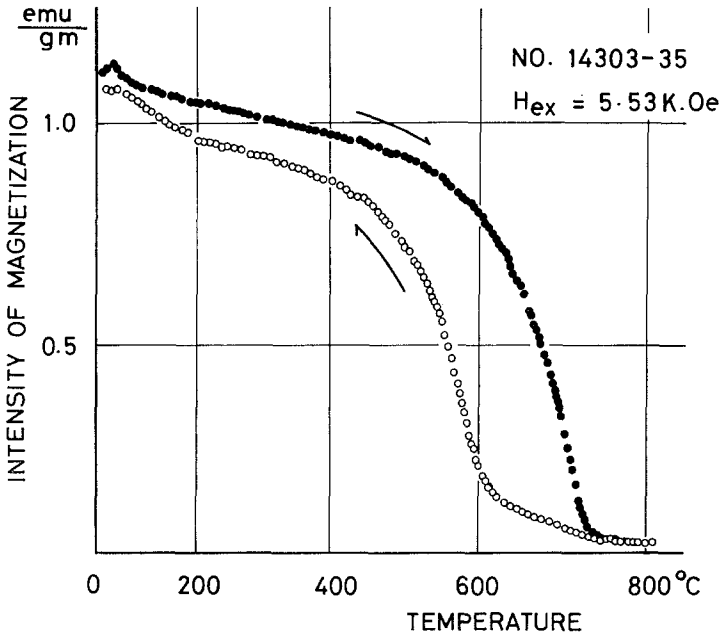

Fig. 4a.

Figs. 4a–b. Magnetization versus temperature curve measured in a magnetic field of 5.53 K Oe. Full circles- : heating process; hollow circles- : cooling process; Sample 14303–35. (a) the first run measurements; (b) the second run measurements.

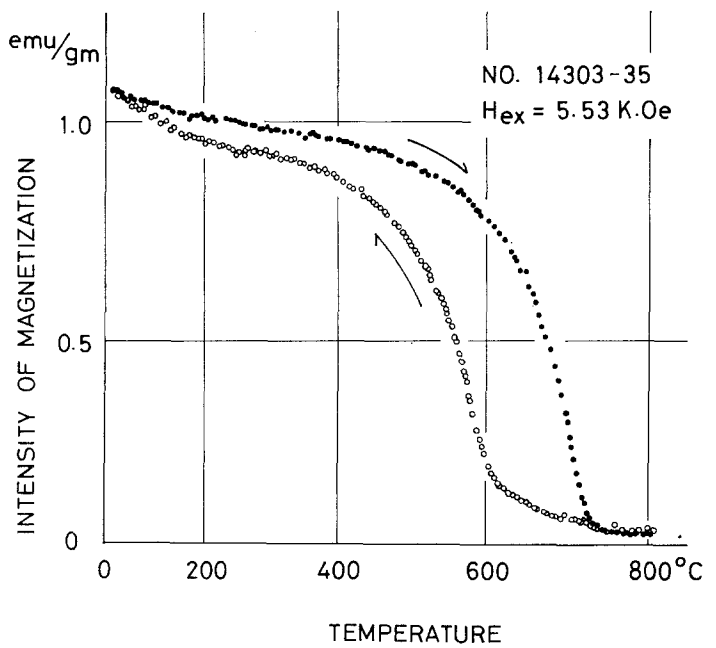

Fig. 4b.

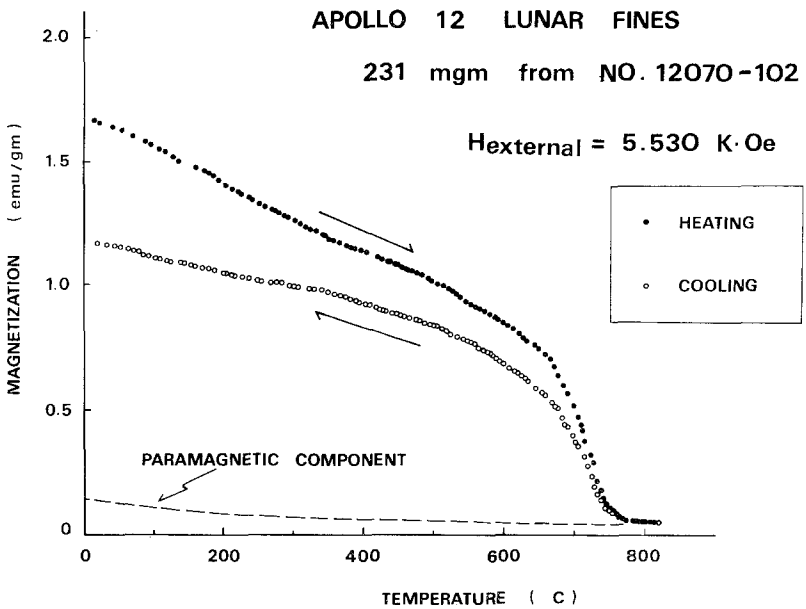

Fig. 5. Magnetization versus temperature curve measured in a magnetic field of 5.53 K Oe. Sample 12070–102 (Fines).

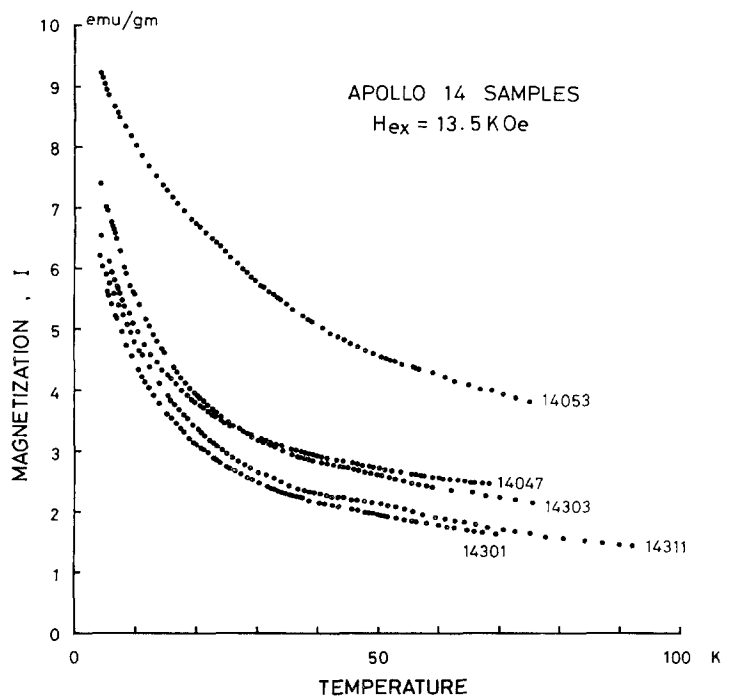

Fig. 6. Magnetization versus temperature curve for the temperature range between 5 and 100 K in a magnetic field of 13.5 K Oe. Numerals in figures represent sample numbers.

The observed decrease in Curie point temperature might possibly be attributed to either a certain small content of silicon in FeSi alloys or that of nickel in FeNi alloy (Bozorth, 1951).

In Table IV, all reported values of Curie point temperature of Apollo 11 and 12 materials are summarized. Θ_c values in this table range from 750 °C to 788 °C. Curie point temperature of Apollo 11 fines, No. 10084, were measured independently by four research teams in addition to ours. The observed values of Θ_c of this sample range from 760 °C to 778 °C. The dispersion of the observed values of Θ_c may imply the heterogeneity of composition of native irons within a returned pack of the Apollo 11 fines as well as possible errors in measurements by different investigators. The same argument could be applied to Apollo 12 fines, No. 12070, and Apollo 11 breccia, No. 10048. Generally speaking, the observed values of Curie point temperature of Apollo lunar materials are not drastically different from that of metallic iron, whence one may approximately conclude that *the dominant ferromagnetic component in the lunar materials is nearly pure metallic iron.*

In regard to further details of the composition of the lunar metallic iron, more direct and comprehensive examinations of separated metallic iron grains will have to

TABLE IV

Curie temperature (Θ_c) and saturation magnetization (I_s) of Apollo 11 and 12 lunar materials

Sample number	Author	Θ_c	I_s
		(°C)	(emu/g)
(Igneous rocks)			
10069	Helsley (1970)	752	–
10024–22	Nagata *et al.* (1970)	755 ± 5	0.155
12002	Helsley (1970)	770	–
12022	Helsley (1970)	770	–
12018–47	Runcorn *et al.* (1970)	770	–
12020–23	Runcorn *et al.* (1970)	770	0.52
12052–48	Grommé and Doell (1971)	788	–
12065–37	Grommé and Doell (1971)	782	–
12053–47	Nagata *et al.* (1971)	760 ± 8	0.195
(Fines)			
10084–86	Doell *et al.* (1970)	770	–
10084–13	Runcorn *et al.* (1970)	778 ± 3	1.6
10084–90	Strangway *et al.* (1970)	776	1.13
10084–88	Schwarz (1970)	770	1.15
10084–89	Nagata *et al.* (1970)	775 ± 5	1.17
12070–103	Runcorn *et al.* (1971)	776	1.8
12070–104	Strangway *et al.* (1971)	770	0.68
12070–102	Nagata *et al.* (1971)	770 ± 8	1.28
(Breccias)			
10048–22	Laroschell and Schwarz (1970)	750	–
10048–55	Nagata *et al.* (1970)	765 ± 5	1.8
10059–24	Doell *et al.* (1970)	775	2.15

be required, though several possibilities can be pointed out based on the existing data. For instance, the irreversible cycle of magnetization with respect to temperature change and a definite reduction of Curie point temperature of Sample 14303–35, illustrated in Figure 4, seems to imply that the principal component of native irons in this sample is FeNi alloy, very likely a kamacite of about 7% of Ni content. Actually, FeNi alloys have been found as the native irons in the lunar fines and breccias (e.g. Mason and Melson, 1970; Levinson and Taylor, 1971). As Strangway *et al.* (1970) have shown from their study in detail on Apollo 11 breccia 10084–90, individual grains of native iron in the lunar material could have different chemical compositions, for example, different ratios of Ni/Fe in different grains. In other words, the *I-T* curve of a bulk sample, such as illustrated in Figure 4, could be a superposition of a large number of individual *I-T* curves of different characteristics. Actually, samples 14301–65 and 14311–45 have almost the same characteristics of irreversible cycle as that of 14303–35, but Curie point temperature is definitely higher (by about 15 °C) in the former two than in the latter. In this regard, there is a possibility that a reduction of Curie temperature is mainly due to a formation of FeSi alloy, since the abundance of silicon is sufficiently high in all lunar materials. Grommé and Doell (1971) have pointed out, on the other hand, that Curie temperatures of samples 12052–48 and 12065–37, which are significantly higher than Θ_c value of pure iron, could be attributed to FeCo alloy of about 1.2% in cobalt content. The effect of Co content on Θ_c also is highly probable, because an appreciable amount of Co has been found in the native irons in the lunar materials. (e.g. Nagata and Carleton, 1970). We may thus have to consider, at least, the system of Fe–Ni–Co–Si as a probable composition of native irons in the lunar materials. As far as data given in Table I through IV are concerned, the average value of Θ_c of the lunar igneous rocks is (768.2 ± 3.5) °C, while that of the lunar fines and breccias is (762.5 ± 3.4) °C. Although the average Curie point temperature of the lunar igneous rocks is a little closer to the value of Θ_c of pure iron than that of the fines and breccias, the difference may not be regarded highly significant at the present stage of statistics. A tentative conclusion about the ferromagnetic substance in the lunar materials would therefore be that Fe is absolutely dominant with a slight amount of Ni and Co, and probably Si also, in the lunar native irons, as indicated by the range of dispersion of Θ_c from 735 °C to 788 °C.

3. Paramagnetic and Antiferromagnetic Components in the Lunar Materials

As given in Tables I through III, the apparent magnitude of paramagnetic susceptibility (χ_a) of the lunar materials at 300 K amounts to $(2.1 \sim 4.6) \times 10^{-5}$ emu/g. The apparent value of χ_a represents not only that of the pure paramagnetic component mostly due to Fe^{2+} in pyroxenes but also the susceptibility of antiferromagnetic components such as ilmenite ($FeTiO_3$), troilite (FeS) and probably ferrosilite ($FeSiO_3$) and/or pyroxferroite ($Ca_{0.15}Fe_{0.85}SiO_3$) whose magnetic properties have not yet been determined.

Experimental endeavour has been made to detect Néel point transition (at 320 °C)

of troilite whose presence is known in the lunar materials, but no evidence of its presence has been detected in the *I-T* curves of the lunar materials within a limit of experimental errors. The antiferromagnetic FeS may therefore be neglected in analyzing the magnetization versus temperature curves of the lunar materials. Then, Néel points of all other antiferromagnetic components are considerably lower than room temperature. Hence, the apparent value of χ_a observed at room temperature (T_0) may be expressed as

$$\chi_a(T_0) = m_0 \frac{C_0}{T_0} + \sum_i m_i \frac{C_i}{T_0 - \Theta_i}, \tag{3}$$

where T_0 and Θ_i denote respectively absolute temperature (300 K) and paramagnetic Curie temperature of i-th antiferromagnetic component; m_0 and m_i represent respectively mass abundances of the paramagnetic component and i-th antiferromagnetic one, and C_0 and C_i are Curie constants of the paramagnetic component and i-th antiferromagnetic one respectively. In the present case, antiferromagnetic Néel points of ilmenite ($\Theta_i = 57$ K, Ishikawa and Akimoto 1958) and ferrosilite ($\Theta_i = 30$ K; Sawaoka *et al.*, 1968) have been detected (Nagata *et al.*, 1970) but the minoralegically detected pyroxferroite might also be antiferromagnetic because $Mg_xFe_{1-x}SiO_3$ is antiferromagnetic for a range of $0 \leq \chi \lesssim 0.25$ (Shenoy *et al.*, 1969).

If, as a rough approximation, we can assume that χ_a represent an apparent paramagnetic susceptibility of the whole iron oxides, expressed as $\chi_a(T) = \bar{m}\,\bar{C}/T$, with an assumption of $\Theta_i \ll T_0 = 300$ K, then $\bar{m}\,\bar{C}$ can be estimated from the observed values of χ_a listed in the tables as $\bar{m}\,\bar{C} = (0.6 \sim 1.4) \times 10^{-2}$ emu/g.

Among metallic irons in the lunar materials, only Fe^{2+} and Mn^{2+} can play role in the paramagnetic behavior, because no Fe^{3+} has been detected in them. Since further the content of Mn^{2+} is much less than that of Fe^{2+} in them, we may approximately consider that the whole paramagnetic susceptibility observed at 300 K is due to Fe^{2+} in pyroxenes, ilmenites and other Fe^{2+}-bearing minerals. Then χ_a can be expressed by

$$\chi_a = \frac{\bar{m} N_A}{3kT_0} \mu_0^2 P_B^2(Fe^{2+}), \tag{4}$$

where μ_B and $P_B(Fe^{2+})$ denote respectively the magnetic moment of Bohr magneton and Bohr magneton number of Fe^{2+} which is 5.39 on average, while k and N_A are the Boltzmann constant and Avogadro number. Putting numerical figures into μ_B, $P_B(Fe^{2+})$, k and N_a, (4) becomes

$$\chi_a = \bar{m} \frac{6.45 \times 10^{-2}}{T_0} \text{ emu/g}, \tag{4'}$$

whence the weight content of Fe^{2+} in the lunar materials is estimated to be $9 \sim 22\%$, or in other words, the weight content of FeO is $12 \sim 28\%$. These estimated values of FeO content certainly give the upper limit, because the equivalent value of C_i for Fe^{2+} ion in ilmenite and ferrosilite is $15 \sim 30\%$ larger than C_0 at temperatures higher

than their Néel points. A more reasonable estimate of contents of Fe^{2+}, $FeTiO_3$ and possible $FeSiO_3$ (or $(Fe_{1-x}Ca_x)\,SiO_3$) in the lunar materials may require analyses of the magnetization versus temperature curves for the low temperature range (from 5 K to 300 K), such as illustrated in Figure 6. The magnetization, $I(T)$, in Figure 6 may be approximately represented by a sum of a paramagnetic component of pyroxene $\chi_{px}(T)\,H$, antiferromagnetic components of ilmenite, $\chi_{Il}(T)\,H$, and ferrosilite $\chi_{Fr}(T)\,H$, and ferromagnetic component of metallic iron $I_F(H)$: namely,

$$I(T) = \{m_{px}\chi_{px}(T) + m_{Il}\chi_{Il}(T) + m_{Fr}\chi_{Fr}(T)\}\,H + m_F I_F(H), \tag{5}$$

where m_{px}, m_{Il}, m_{Fr} and m_F represent respectively the weight contents of paramagnetic pyroxene, ilmenite, ferrosilite and metallic iron. Since the functional forms of $\chi_{px}(T)$, $\chi_{Il}(T)$ and $\chi_{Fr}(T)$ with respect to T have been known experimentally (Stickler *et al.*, 1967; Sawaoka *et al.*, 1968), and $I_F(H)$ can be considered independent of temperature in the low temperature range, the best fitting simulation curve expressed by (5) for the observed $I(T)$-T curves can derive the weight contents of the four magnetic constituents. This simulation method was fairly successful in analyzing Apollo 11 lunar materials (Sample 10024–22, and 10048–55), in which the content of $FeTiO_3$ is unusually high; m_{px}, m_{Il}, m_{Fr} and m_F thus derived from the $I(T)$-T curve is in fairly good agreement with the result of chemical and mineralogical analyses of the same sample (Nagata *et al.*, 1970). Even in the best case (Sample 10024–22) however, a considerable discrepancy between the observed curve and the simulated one cannot be eliminated for a temperature range from 10 K to 40 K. In all other examples (7 in total number) of similar magnetic analyses by use of (5), the simulated values become considerably smaller than the observed values only for a temperature range between 10 K and 40 K. This general tendency of discrepancy may suggest that antiferromagnetic phases having their Néel point between 10 K and 40 K are present in the lunar materials. Mössbauer analyses made by Shenoy *et al.* (1919) have shown that the spin configuration in $(Mg_xFe_{1-x})\,SiO_3$ is in the ordered state for a range of x from 0 to 0.25, and the corresponding Néel points range from 37 K to 11 K. Since pyroxferroite $(Ca_xFe_{1-x})\,SiO_3 (x \sim 0.15)$ must have a similar spin configuration as $(Mg_xFe_{1-x})\,SiO_3$, there is a considerable possibility that pyroxferroite and other pyroxenes are in antiferromagnetic states having Néel points in 10 K–40 K temperature range. It seems that the result of magnetic analysis of the lunar materials by use of (5) cannot be sufficiently accurate without knowledge of magnetic properties of all possible pyroxene phases, except a special case that Néel point peaks of $FeTiO_3$ and $FeSiO_3$ are clearly observed. In this regard, studies on magnetic properties of pyroxenes of various chemical compositions will be highly necessary in the future.

However, a method to estimate an approximate abundance of ilmenite from the $I(T)$-T curves will be newly proposed. The magnetization $I(T)$ in a constant magnetic field for a temperature range higher than Néel points may be represented by

$$I(H, T) = m_0 H \frac{C_0}{T} + H \sum_i m_i \frac{C_i}{T - \Theta_i} + m_F I(H), \tag{6}$$

where the definitions of symbols are same as in (3) and (5). Differentiating (6) with respect to $(1/T)$, we get

$$\frac{\partial}{\partial(1/T)} I(H, T) = m_0 H C_0 + H \sum_i m_i \frac{C_i}{(1 - \Theta_i/T)^2}, \quad (T \geq \Theta_i), \tag{7}$$

where the terms of antiferromagnetic components only are temperature dependent. Consider here an antiferromagnetic component at temperatures a little higher than its Néel point. The antiferromagnetic term, $C_i/(1-\Theta_i/T)^2$ is positive and it decreases with an increase in temperature. At temperatures a little lower than Néel point, the susceptibility $\chi(T)$ sharply increases with temperature in an approximate mathematical form expressed by

$$\chi(T) \simeq \frac{C_i'}{(T_c + \theta - T)}, \quad (T \leq T_c), \tag{8}$$

where T_c represents Néel point temperature, and C_i' and θ are positive constants which satisfy the condition

$$C_i'/\theta = C_i/(T_c - \Theta_i) = \chi(T_c).$$

Then,

$$\frac{\partial}{\partial(1/T)} \chi(T) = -\frac{C_i' T^2}{(T_c + \theta - T)^2}, \quad (T \leq T_c), \tag{9}$$

which is of a negative value. Thus $\partial\chi(T)/\partial(1/T)$ discontinuously jumps up at Néel point temperature from $-C_i T_c^2/(T_c - \Theta_i)\,\theta$ to $+C_i T_c^2/(T_c - \Theta_c)^2$, and then it gradually decreases with T. If we roughly assume $C_i' = C_i$, then $\theta = T_c - \Theta_i$. Then, the magnitude of discontinuous jump of $\partial I(T)/\partial(1/T)$ at T_c is given by

$$\left[\frac{\partial I(T)}{\partial(1/T)}\right]_{T=T_c} \simeq \frac{2 m_i C_i H}{(1 - \Theta_i/T_c)^2} = 2 m_i H T_c^2 \chi^2(T_c)/C_i. \tag{10}$$

Since C_i and $\chi(T_c)$ have been determined for a known antiferromagnetic phase, one can approximately estimate the weight content m_i from the discontinuous jump in a $\partial I(T)/\partial(1/T)$ curve.

Figure 7 illustrates two examples of $\partial I(T)/\partial(1/T) \sim T$ curves computed from $I(T) \sim T$ plots of the lunar materials. A sharp jump of $\partial I(T)/\partial(1/T)$ value takes place at Néel point temperature (57 K) of ilmenite in both cases. Since $\chi(T_c) = 7 \times 10^{-4}$ emu/g and $C_i = 2.7 \times 10^{-2}$ (emu/g) K for ilmenite, (10) is numerically expressed for ilmenite as

$$\left[\frac{\partial I(T)}{\partial(1/T)}\right]_{T=57\,\mathrm{K}} \simeq 0.11\, m_i H\ (\mathrm{emu/g})\mathrm{K}. \tag{10}'$$

Estimates of m(ilmenite) with the aid of (10)′ from data shown in Figure 7(a) and (b) are 7 weight percent in sample 10048–55 and 3 weight percent in Sample 14311–45, respectively.

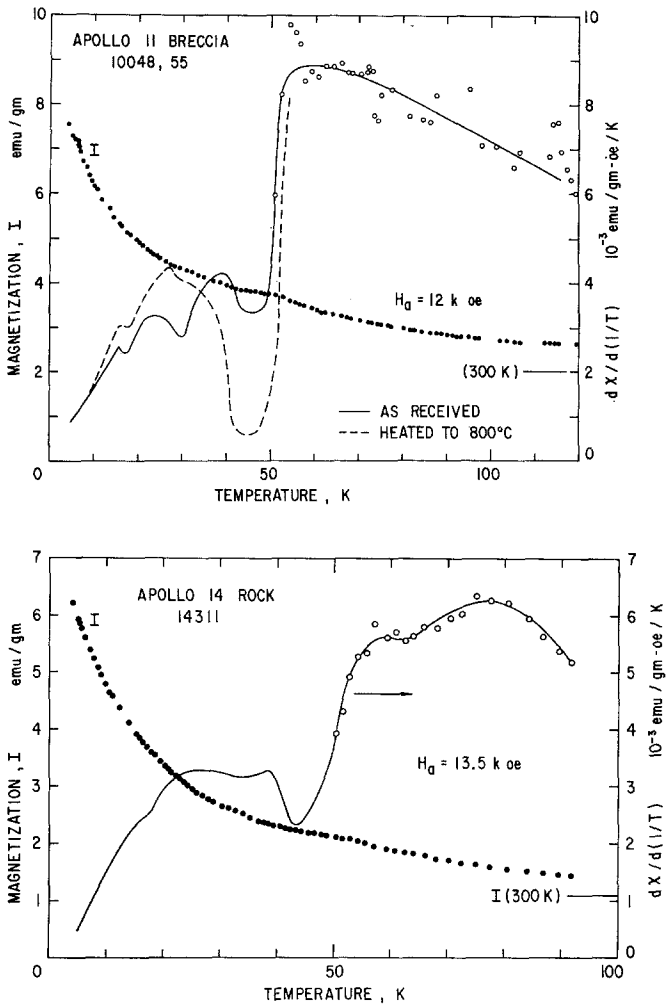

Fig. 7. Examples of the magnetization (I) versus temperature (T) curve for the low temperature range and the corresponding relationship between $\partial I/\partial(1/T)$ and T.

4. Viscous Magnetization and Very Fine Grains of Metallic Iron in the Lunar Materials

One of remarkable magnetic characteristics of the lunar materials, summarized in Table I through Table III, may be that H_{RC} is extremely larger than H_c, particularly in the lunar fines and breccias. The ratio H_{RC}/H_c exceeds 3.6 even in the lunar igneous rocks and it becomes larger than 10 in the lunar fines.

The coercive force and the remanence coercive force of terrestrial basalts and synthesized titanomagnetite powders have been extensively studied by Wasilewski (1969). His results have shown that

$H_c = (0.75 \pm 0.025) H_{RC}$ for small grain titanomagnetite in basalt,
$H_c = (0.54 \pm 0.03) H_{RC}$ for large grain titanomagnetite in basalt,
$H_c \simeq 0.50\ H_{RC}$ for fresh synthesized titanomagnetite,
$H_c \simeq 0.66\ H_{RC}$ for synthesized titanomagnetite after heating at 600 °C.

In any case, $H_{RC}/H_c \lesssim 2$ for terrestrial basalts and synthesized titanomagnetites. As discussed by Wohlfarth (1963), for example, the theoretical value of H_{RC}/H_c for a random assemblage of non-interacting uniaxial particles amounts only to 1.094. Gaunt (1960) has theoretically estimated the maximum possible value of this ratio when the particle size has a distribution spectrum and therefore the intrinsic coercive force (H_c) of individual particle is subjected to its distribution function $f(H_c)$. His theoretical result has given that

$$(H_{RC}/H_c) \leqq 2.02,$$

and actually he experimentally obtained $(H_{RC}/H_c) = 2$ for dilute AuCo alloys.

It has thus been concluded that the ratio H_{RC}/H_c of a dilute assemblage of ferromagnetic (or ferrimagnetic) particles is between unity and 2 in the ordinary case. In this regard, the observed values of H_{RC}/H_c of the lunar materials must be considered abnormally large. As discussed generally by Wohlfarth (1963) and others, the abnormal value of H_{RC}/H_c of an assemblage of ferromagnetic particles can be attributed only to a superposition of a superparamagnetic component (or a magnetically very soft component) on a magnetically hard component which is associated with the remanent magnetization (I_R). We may consider that a ferromagnetic magnetization $I_F(H)$ can be represented by a sum of the magnetization of a hard component, $I_H(H)$, and that of a soft component, $I_s(H)$: namely,

$$I_F(H) = (1 - \alpha)\, I_H(H) + (\alpha)\, I_s(H), \tag{11}$$

where $\alpha < 1$ denotes the weight content of the soft component, and where we can approximately assume that $I_s(H)$ component has no remanent magnetization at room temperature, i.e. $I_s(H=0) = 0$. Then, $I_F(H=0) = I_R = (1-\alpha) I_H(H=0)$, and H_{RC} is exactly the same as the remanence coercive force of the hard component. When $H = -H_c$, (11) becomes

$$(1 - \alpha)\, I_H(H = -H_c) = \alpha I_s(H_c). \tag{12}$$

It means that H_c is the same as the coercive force (H_c^0) of the hard component for $\alpha = 0$ and $H_c = 0$ for $\alpha = 1$, and H_c decreases with an increase of α. Thus, the ratio H_{RC}/H_c can increase with an increase of α from zero to unity. Quantitative features of H_{RC}/H_c of the lunar materials are not discussed here but will be published elsewhere. However, the fact that the superparamagnetically soft component (I_F) at room temperature becomes blocked at a very low temperature is seen in Table V, where the magnetic parameters, χ_a, I_s, I_R, H_c and H_{RC}, of the lunar materials measured at both 300 K and 5 K (12.5 K for Sample 14311–45) are summarized. In those samples whose H_{RC}/H_c ratio at room temperature is extremely large (Samples, 10048–55, 14047–47, and 14259–69) H_c and I_R at the low temperature becomes much larger than those at

room temperature, and the ratio H_{RC}/H_c approaches to 2 at the low temperature. The marked increase of H_c and I_R obviously indicates the blocking of superparamagnetically fine iron particles at the low temperature.

TABLE V

Magnetic parameters of lunar materials measured at room temperature and at very low temperature with type of VRM

Sample No.		χ_a (emu/g)	I_s (emu/g)	I_R	H_c (Oe)	H_{RC}	Type of VRM	Fe(after)[a] / Fe(before)
10048–55	300 K	4.3×10^{-5}	1.8	13×10^{-2}	50	500	II	0.64
	5 K	36.2×10^{-5}	3.0	54×10^{-2}	190	500		
14047–47	300 K	2.4×10^{-5}	1.4	6.1×10^{-2}	26	350	II	0.67
	5 K	32×10^{-5}	2.1	32×10^{-2}	175	450		
14053–48	300 K	4.6×10^{-5}	2.2	3.2×10^{-2}	20	80	I	0.97
	5 K	50×10^{-5}	3.0	4.0×10^{-2}	21	–		
14130–65	300 K	2.1×10^{-5}	0.69	0.64×10^{-2}	27	500	II	0.86
	5 K	33×10^{-5}	1.45	–	–	–		
14303–35	300 K	2.4×10^{-5}	1.27	2.1×10^{-2}	27	180	I	0.97
	5 K	42×10^{-5}	1.73	3.4×10^{-2}	33	–		
14311–45	300 K	2.3×10^{-5}	0.74	0.43×10^{-2}	17	140	I	0.97
	12.5 K	38×10^{-5}	1.2	–	–	–		
14259–69	300 K	2.5×10^{-5}	1.5	6.0×10^{-2}	19	300	II	0.67
	5 K	31×10^{-5}	2.6	44×10^{-2}	140	350		

a Remarks: Fe(after) = Content of metallic iron after heating to 820° C in 10^{-5} T atmospheric pressure.
Fe(before) = Content of metallic iron of fresh sample.

It has been reported, on the other hand, that some lunar materials contain an extremely soft magnetic component which causes a considerably large amount of the viscous remanent magnetization (VRM) by exposing the rock samples for a little while to the geomagnetic field (Nagata *et al.*, 1970; Larochelle and Schwarz, 1970; Doell *et al.*, 1970; Nagata and Carleton, 1970; Nagata *et al.*, 1971). The bulk magnetic properties of the lunar fines have generally shown that the soft and viscous magnetic component is particularly dominant in the lunar fines. Nagata *et al.* (1970) quantitatively have shown, for example, that the superparamagnetic component originating in fine grains (about 10^2 Å in mean diameter) of native irons occupies a little over a half of the metallic irons in Apollo 11 lunar fines. Lunar breccias (or fragmented rocks) also contain a considerable amount of the soft and viscous magnetic component if they have not been strongly impact-metamorphosed. (Nagata and Carleton, 1970; Nagata *et al.*, 1971).

The presence of a considerable amount of such fine grains of metallic irons in the lunar fines and breccias has been recognized also from an observed fact that these rock samples lose a considerably large portion of their ferromagnetic component by heating them up to 800 °C even in a reasonably high vacuum of $10^{-6}\sim10^{-5}$ T of atmospheric pressure: the loss of the ferromagnetic component is interpreted as due to the oxidation of very fine grains of metallic iron (Nagata *et al.*, 1970).

On the contrary, the soft and viscous component of ferromagnetics occupies only a small portion of the total ferromagnetics in the lunar igneous rocks. In fact, changes in the total amount of ferromagnetic component in the igneous rocks by heating to 800 °C in $10^{-6} \sim 10^{-5}$ T atmosphere are generally very small.

As a preliminary step to classify the two distinctly different types of viscous magnetic characteristics of the lunar materials, it has been tentatively proposed (Nagata and Carleton, 1970) that the ratio of VRM acquirable in the geomagnetic field (the field intensity $H=0.6$ Oe) during an infinitely long time, ΔI_V, to the stable component of NRM, I_0, namely $\Delta I_V/I_0$, could be adopted as a parameter to evaluate the relative magnitude of viscous magnetic component in the total ferromagnetic substance. The definition of ΔI_V is made for the acquisition of VRM during an infinitely long time, but practically it can be estimated with a sufficient reliability by exposing a sample to the geomagnetic field during one full day or so. The parameter $\Delta I_V/I_0$ has been used for a criterion to judge whether an observed NRM is mostly due to the real remanent magnetization acquired on the lunar surface or mostly due to VRM acquired in the geomagnetic field since the time of its return to the Earth. The cases of $\Delta I_V/I_0 \ll 1$ and $\Delta I_V/I_0 \gtrsim 1$ may be called Type I and Type II respectively of viscous magnetic character. Figures 8 and 9 illustrate examples of Type I and Type II respectively of VRM of the lunar materials. In these diagrams, the time-decay of viscous magnetic component of IRM in a non-magnetic space is demonstrated. Since the intensity of viscous magnetization is approximately proportional to the intensity of a magnetic field applied on a

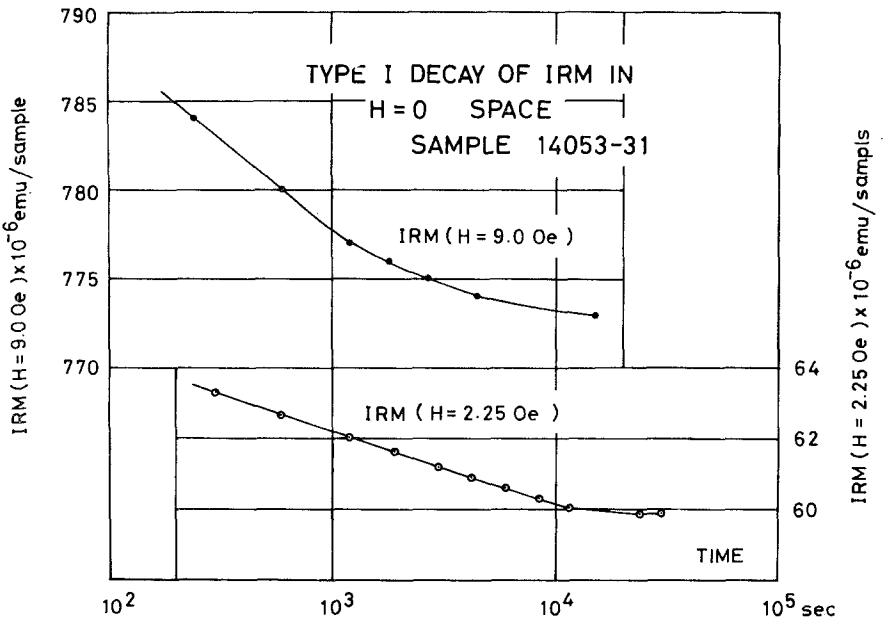

Fig. 8. Two examples of Type I viscous remanent magnetization.

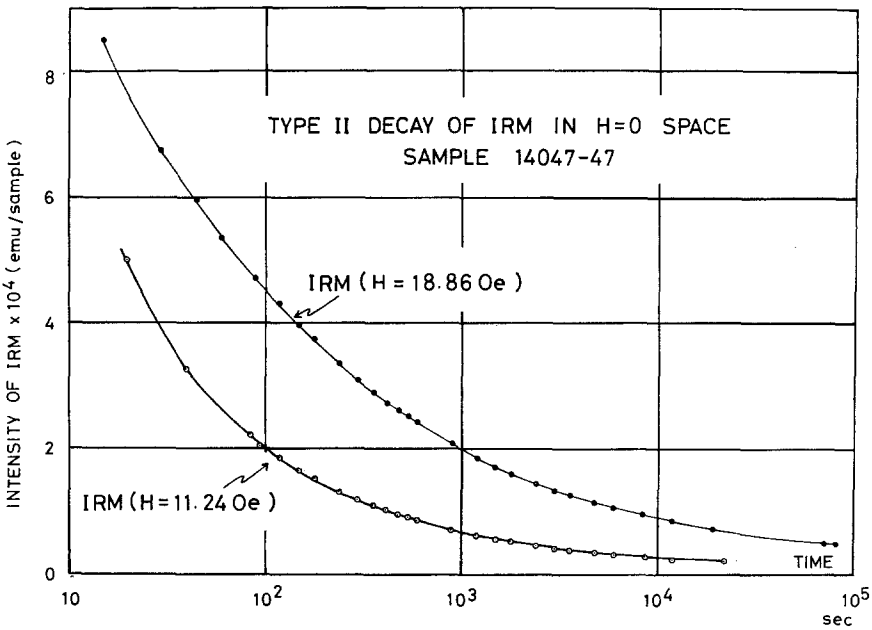

Fig. 9. Examples of Type II viscous remanent magnetization.

sample to acquire IRM, the defined value of ΔI_V at $H=0.6$ Oe can be approximately obtained from these data of the decay of IRM in $H=0$ space. Representing the amounts of viscous and stable components of IRM acquired by $H=0.6$ Oe by ΔI_V^* and I_0^* respectively, it has been generally derived that always $\Delta I_V^*/I_0^* \ll 1$ in Type I materials and $\Delta I_V^*/I_0^* \gtrsim 1$ in Type II materials.

In Table V, the characteristics of magnetic viscosity of measured samples are classified into the two distinctly separated types. In the same table, the ratio of the amount of ferromagnetic component after the heat treatment to 820 °C to that of the fresh sample also in given. It is observed in the table that Type II samples have a large value of $H_{RC}/H_c(>10)$, a large value of $I_R(5\text{ K})/I_R(300\text{ K})$ (>4), and a large value of $H_c(5\text{ K})/H_c(300\text{ K})$ (>4) and the ratio Fe(after)/Fe(before) is smaller than 0.86, while Type I samples have a smaller value of $H_{RC}/H_c(<8)$, a smaller value of $H_c(5\text{ K})/H_c(300\text{ K})$ (<2) and a smaller value of $I_R(5\text{ K})/I_R(300\text{ K})$ (<1.2), and the ratio Fe(after)/Fe(before) is close to unity.

It may thus become clear that Type II lunar rocks contain a considerable amount of very fine grains of metallic iron which behave superparamagnetically at room temperature. Needless to say, the viscous magnetic component must be completely washed away for the purpose of paleomagnetic studies of the lunar rocks, particularly in case of Type II rocks, in which the viscous magnetization is dominant.

From the viewpoint of lunar rock magnetism, the superparamagnetically soft component in the lunar materials may have to be examined in more detail in terms of

the grain size of metallic iron. In general, the viscous decay of remanent magnetization (I) in $H=0$ space with time (t) can be expressed by

$$I(t) = I_0 + \int_0^\infty \varphi(\tau)\, e^{-t/\tau}\, d\tau, \tag{13}$$

where I_0, τ and $\varphi(\tau)$ denote respectively the stable component of magnetization, the relaxation time for the decay of soft magnetization and the distribution spectrum of magnetic particles with respect to τ. As already discussed (Nagata and Carleton, 1970), $I(t)$ in case of VRM-Type I sample can be approximately represented by a line spectrum or two or three line spectra of τ, namely,

$$I(t) = I_0 + \sum_i \Delta I_i e^{-t/\tau_i}, \quad (i \leq 3). \tag{13'}$$

For example, $\tau = 1.35 \times 10^3$ s, $\Delta I = 2.6 \times 10^{-6}$ emu/g and $I_0 = 146.5 \times 10^{-6}$ emu/g for IRM($H=9.0$ Oe) of Sample 14053–31; and $\tau_1 = 5.2 \times 10^2$ s, $\tau_2 = 4 \times 10^3$ s, $\Delta I_1 = 5.0 \times 10^{-7}$ emu/g, $\Delta I_2 = 3.1 \times 10^{-7}$ emu/g, and $I_0 = 251 \times 10^{-7}$ emu/g for IRM($H=16.9$ Oe) of Sample 14303–35.

For $I(t)$ of VRM-Type II samples, the well-known Richter model of the magnetic after-effect (e.g. Becker and Döring 1939) represented by

$$I(t) = I_0 + \Delta I \int_{\tau_1}^{\tau_2} \left(\frac{1}{\tau \ln(\tau_2/\tau_1)} \right) e^{-t/\tau}\, d\tau, \tag{14}$$

seems to be applicable. Actually, (14) has been successfully applied on analyzing the magnetic viscous decay of lunar breccias 10021–32 and 10048–55: $\tau_1 = 3.5 \times 10^2$ s and $\tau_2 = 7 \times 10^4$ s for Sample 10021–32, and $\tau_1 = 10$ s and $\tau_2 = 2.2 \times 10^5$ s for Sample 10048–55. However, the simple functional form of (constant/τ) for $\varphi(\tau)$ in (13) is not sufficient for analyzing the magnetic viscous decay of Type II lunar samples which contain much abundance of extremely fine grain of metallic iron such as Sample 14047 (Figure 9) and 14301. A more generalized method of analyzing the viscous magnetic decay of such cases will be proposed in the followings.

Even the sharp viscous decay of $I(t)$ with time, such as illustrated in Figure 9, which cannot be represented by (14), can be empirically expressed by

$$I(t) = I_0 + \frac{C}{(t + t_0)^\nu}, \tag{15}$$

where C, t_0 and ν are empirical constants. The viscous component, $I(t) - I_0$, is C/t_0^ν at $t=0$ and zero at $t=\infty$.

In comparison of (12) with (15),

$$\int_0^\infty \varphi(\tau)\, e^{-t/\tau}\, d\tau = \frac{C}{(t + t_0)^\nu}, \tag{16}$$

the inverse Laplace transform can derive $\varphi(\tau)$ as

$$\varphi(\tau) = \frac{C}{\Gamma(\nu)} \frac{e^{-t_0/\tau}}{\tau^{1+\nu}}, \tag{17}$$

where ν should be positive, and it is always positive empirically. In (17), $\varphi(\tau)=0$ at $\tau=0$ and $\varphi(\tau)=0$ also at $\tau=\infty$. The special case of $t=0$ and $\nu=0$ of (17) is identical to the case of Richter's model. In other words, (17) is a generalized form of the Richter's one, (C/τ). Figure 10 illustrates the spectral forms of $\varphi(\tau)$, obtained with the aid of (15) and (17), for IRM's acquired in $H=16.86$, 11.24 and 5.62 Oe of magnetic field for sample 14047–47. As seen in the figure, each spectrum, $\varphi(\tau)$, has a high peak in the range of $0<\tau<10$ s in Sample 14047. With an increase in H for IRM, the contribution of fine particles of larger value of τ to the viscous magnetization increases, and the spectral peak shifts towards a larger value of τ. It may be worthwhile to note here that I_0 increases parabolically with H, but C increases almost linearly with H, as predicted theoretically. A similar result of analysis has been obtained for the spectral form of $\varphi(\tau)$ of Sample 14301–60 also, but the peak of $\varphi(\tau)$ around $\tau=10$ s is much higher than the case of Sample 14047.

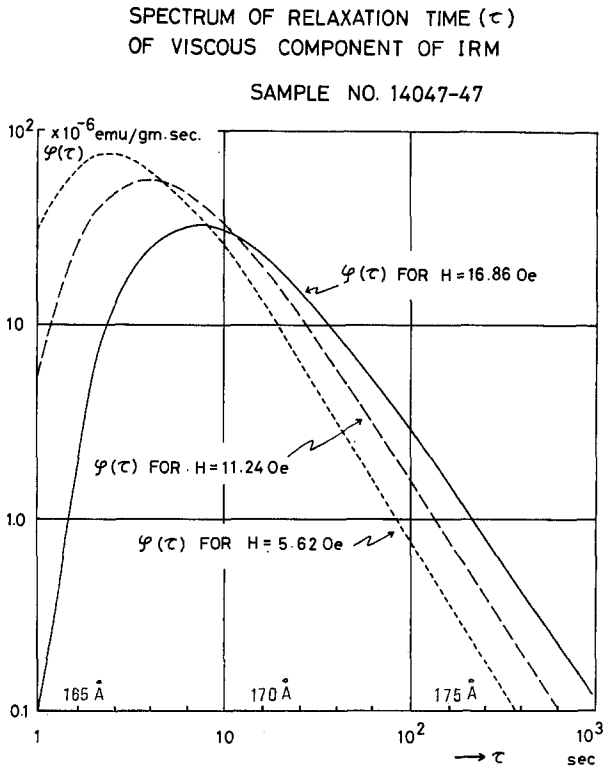

Fig. 10. The distribution of spectra of fine grains of metallic iron with respect to their relaxation time (τ).

The relationship between τ and the grain size of a single domain particle of ferromagnetics has been reasonably well formulated by Néel (1949) as

$$\frac{1}{\tau} = f_0 \exp\left(-\tfrac{1}{2} H_{RC} J_s^0 \bar{v}/kT\right), \tag{18}$$

where $\bar{v}$, J_0^s and f_0 represent respectively the average volume of fine ferromagnetic grains concerned, their spontaneous magnetization per unit volume and an approximately constant coefficient of about $10^9\ s^{-1}$ in magnitude. When the magnitude of H_{RC} is determined for an individual sample, $\bar{v}$ can be estimated from τ in (18), because J_0^s is represented by the spontaneous magnetization of metallic iron as discussed in Section 2. For Sample 14047–47, the mean diameters thus estimated of spherical irons corresponding to different values of τ are given on the abscissa in Figure 10, where the fine iron grains of 160 ~ 170 Å in mean diameter are dominant. In Apollo 11 breccias, Samples 10021–32 and 10048–55, the mean diameter of the very fine grains of metallic iron has been estimated with the aid of (18) to range between 170 and 185 Å and between 160 and 180 Å respectively.

In concluding the viscous magnetic properties of the lunar materials, we may summarize its various characteristics in the following list (Table VI).

5. Stability of Natural Remanent Magnetization of Lunar Rocks and Remarks on a Strongly Magnetic Lunar Igneous Rock

It has already been reported (e.g. Doell *et al.*, 1970; Runcorn *et al.*, 1970; Nagata and Carleton, 1970) that some lunar breccias have a very stable component of the natural remanent magnetization (NRM) which can hardly be AF-demagnetized by applying

TABLE VI

Characteristics of Type I and Type II of VRM of the lunar materials

Observed elements	Type I	Type II
(a) (VRM)/(NRM)	$\Delta I_V/I_0 \ll 1$	$\Delta I_V/I_0 \gtrsim 1$
(b) (Viscous IRM)/(Stable IRM)	$\Delta I_V^*/I_0^* \ll 1$	$\Delta I_V^*/I_0^* \gtrsim 1$
(c) Dependence of VRM on time	$\Delta I_V(t) = \Delta I \exp(-t/\tau)$	$\Delta I_V(t) = C \int_0^\infty (e^{-t_0/\tau}/\tau^{1+p})\, e^{-t/\tau}\, d\tau$
(d) Change in I_R with temperature	$I_R(5\text{ K})/I_R(300\text{ K}) < 1.2$	$I_R(5\text{ K})/I_R(300\text{ K}) > 4$
(e) Change in H_c with temperature	$H_c(5\text{ K})/H_c(300\text{ K}) < 2$	$H_c(5\text{ K})/H_c(300\text{ K}) > 4$
(f) Effect of heating	Fe(after)/Fe(before) $\simeq 1$ (Difficult to be oxidized)	Fe(after)/Fe(before) < 0.85 (Easy to be oxidized)
(g) Dominant grain size of Fe	Fine grains occupy only a small portion of total Fe.	Fe particles smaller than 200 Å in diameter are dominant.
(h) Types of Lunar Material	Lunar igneous rocks	Lunar fines and most lunar breccias.

an alternating magnetic field of several hundred Oersteds. It is believed that such a very stable component of NRM of lunar rocks is certainly due to some physical mechanism to produce the stable remanent magnetization in the presence of a weak magnetic field on the lunar surface, very likely due to either the thermoremanent magnetism (TRM) or the shock remanent magnetism (SRM) or their combined effect. However, NRM's of most lunar igneous rocks and many lunar breccias are not so stable against the AF-demagnetization test, even after the superparamagnetically soft component is sufficiently washed away.

Figure 11 shows two examples of the results of AF-demagnetization of Apollo 14 lunar clastic rocks. To represent numerically the degree of stability of NRM against the AF-demagnetization, two parameters have been introduced; the effective AF demagnetization field ($\tilde{H}_0$) which is defined as the intensity of demagnetization field to reduce the intensity to ($1/e$) of its initial value, and the critical AF demagnetization field ($\tilde{H}^*$) which represents the maximum demagnetization field below which the direction of NRM is approximately invariant (within $\pm 10°$ in most cases) (Nagata *et al.*, 1971). In Table VII, the observed values of $\tilde{H}_0$ and $\tilde{H}^*$ of the lunar igneous and clastic rocks are summarized together with the intensity of NRM. The value of h in the table represents the intensity of magnetic field which can produce IRM whose intensity is the same as that of NRM. Except special cases (such as Samples 10085–16, 10048–55 and 14063–47), both $\tilde{H}_0$ and $\tilde{H}^*$ are smaller than 60 Oe and some of them are smaller than even 20 Oe. This comparatively weak coercivity of NRM against the AF demagnetization may imply that the observed NRM cannot be attributed to TRM.

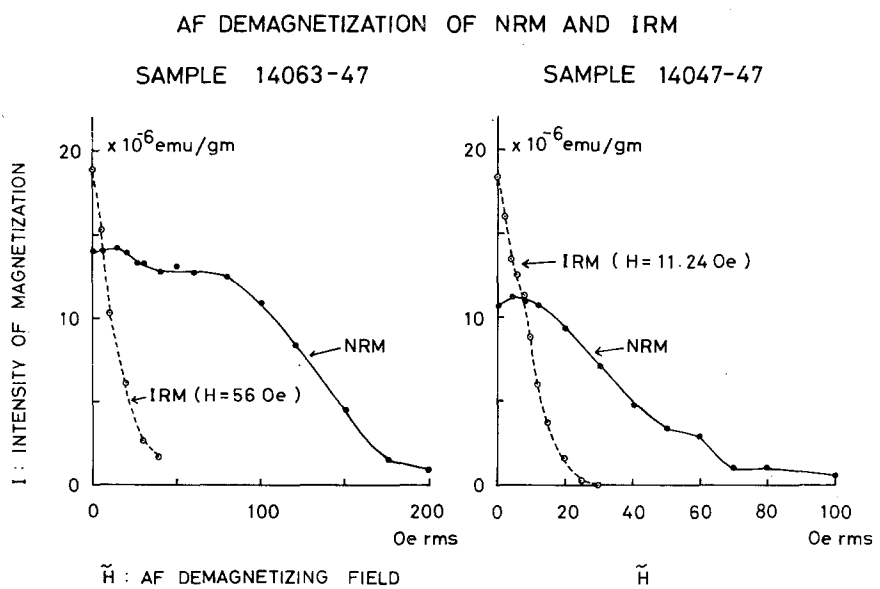

Fig. 11. Two examples of the comparison of AF demagnetization curve of NAM with that of IRM whose intensity is a little higher than that of NRM.

TABLE VII

Natural remanent magnetization and its stability of lunar materials

Sample No.	I_n (emu/gm)	$\tilde{H}_0$ (Oe)	$\tilde{H}^*$ (Oe)	h (Oe)
(Igneous rocks)				
10024–22	7.5×10^{-6}	25	30	14
12053–47	2.3×10^{-6}	8	7	9
12038–29	8.1×10^{-6}	55	40	17
12038–32	6.3×10^{-6}	12	5	15
14053–31	2200.0×10^{-6}	19	80	50
14063–47	14.1×10^{-6}	145	150	47
14310–159	2.4×10^{-6}	> 25	> 25	12
(Breccias or clastic rocks)				
10021–32	15.0×10^{-6}	35	40	–
10048–55	56.0×10^{-6}	~ 400	>100	–
10085–16	153.0×10^{-6}	~ 1400	>500	–
14047–47	8.2×10^{-6}	45	30	7.5
14301–65	41.2×10^{-6}	48	40	23
14303–35	131.2×10^{-6}	18	40	29
14311–23	8.1×10^{-6}	8	10	14

In Figure 11, however, the AF demagnetization curve of the stable component of IRM whose intensity is a little larger than that of NRM of the same sample is shown for comparison. Similar comparisons between NRM and IRM of other lunar igneous rocks and breccias also have indicated that NRM is definitely stabler than IRM of the same intensity against the AF demagnetization. It may therefore be suggested that NRM of these lunar rocks cannot be simply attributed to the acquisition of IRM or similar kinds of artificial remanent magnetization by accident after the samples were returned to the *E*arth's surface.

Another possible test of the stability of NRM would be the thermal demagnetization technique. Figure 12 illustrates an example of the thermal demagnetization curve of an Apollo 14 lunar igneous rock. This curve could be interpreted as a sum of the thermally less stable component represented by a rapid decrease in the lower temperature range and a much smaller portion of the thermally stable component which behaves just as TRM. We may be able to conclude, therefore, that a small portion of NRM of some lunar igneous rock could be attributed to TRM. The very stable component of NRM of Samples 10085–16 and 10048–55 also is believed to be attributable to TRM. Then, the origin of the component of NRM of lunar rocks which is appreciably less stable than TRM but definitely more stable than IRM must be seeked in the future. It seems likely that the shock remanent magnetism accompanied with the TRM effect caused by meteorite impacts could be one of plausible mechanisms.

As shown in Tables I through III and Table VII, Apollo 14 igneous rock sample 14053 is unusually strong in every aspect of its magnetic properties; the content of metallic iron in this particular igneous rock amounts to almost 1 weight percent,

which is as large as that of the lunar fines. The saturation magnetization (I_s) of all other lunar igneous rocks examined so far never exceeds 0.5 emu/g (Runcorn *et al.*, 1970; Nagata *et al.*, 1970; Hargraves and Dorety, 1971; Nagata *et al.*, 1971), which corresponds to the content of metallic iron of about 0.2 weight percent. I_s of the lunar fines and breccias ranges between 0.5 and 2.5 emu/g, but the considerably higher content of metallic iron in them is believed to be caused by mixing of metallic irons of impacting meteorites. On the contrary, Sample 14053 is an igneous crystalline rock (Swann *et al.*, 1971), whence its high content of metallic iron ought to be due to its own mineralogical composition.

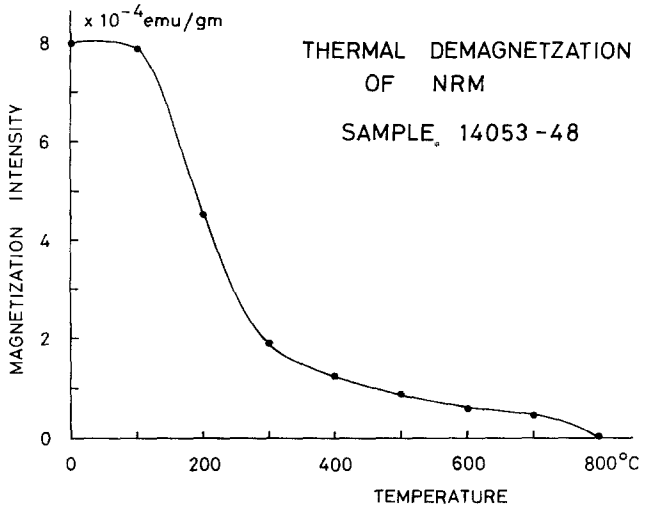

Fig. 12. Example of the thermal demagnetization curve of a lunar igneous rock.

NRM of this sample also is unusually intense, amounting to about 2×10^{-3} emu/g. Two specimens of this rock sample, 14053–31 (5.27 g) and 14053–48 (0.97 g), could be magnetically examined. NRM of Sample 14053–31 is 2.2×10^{-3} emu/g while that of Sample 14053–48 is 2.7×10^{-3} emu/g. A chip (0.304 g in weight) taken from Sample 14053–48 has only 0.80×10^{-3} emu/g in its NRM intensity. Thus, the distribution of NRM intensity within a rock mass of 14053 seems to be appreciably heterogeneous, but still NRM intensity of this sample is unusually large, because NRM intensity of all other lunar igneous rocks so far reported is smaller than 2×10^{-5} emu/g. The unusually intense NRM of this particular sample is primarily due to its unusually high content of metallic iron. An examination of petrological origin of the high content metallic iron in this sample may be desirable. An attention might be called on a possible relationship between a highly magnetized rock mass such as Sample 14053 and the local magnetic anomalies observed at Apollo 14 landing site (Dyal *et al.*, 1970).

6. Concluding Remarks

In the foregoing sections, the magnetic hysteresis curves observed at both 300 K and 5 K, the magnetization versus temperature curves for a temperature range between 5 K and 1100 K, and the viscous magnetic properties of Apollo 11, 12 and 14 lunar materials are critically analyzed. Examinations of Curie point temperature have led to a conclusion that almost pure metallic iron is absolutely dominant as the ferromagnetic constituent in the lunar materials. However, the irreversible cycle of magnetization with temperature, which is similar to the $\alpha-\gamma$ transition of FeNi alloy, and a considerably low value of Curie point temperature as compared with the pure iron one are observed for some lunar rocks. Studies of the effect of Ni, Co, and Si on metallic iron in detail will be necessary in the future work of lunar rock magnetism.

The paramagnetic phase of pyroxenes and the antiferromagnetic phase of ilmenite are clearly observed in all lunar materials. It seems likely, however, that some pyroxene phases, chemically expressed as $(M_xFe_{1-x})SiO_3$ with $M=Ca^{2+}$, Mg^{2+}, etc. may be in the antiferromagnetically ordered state at temperatures below $30\sim40$ K, if x is in the range between 0 and $\frac{1}{4}$. This problem also seems to deserve further studies in detail.

One of striking characteristics of the lunar rock magnetism is the presence of very fine grains of metallic irons of $100\sim200$ Å in mean diameter. The content of such fine grains of metallic irons is considerably large in the lunar fines and breccias, resulting in a marked amount of viscous magnetization or superparamagnetic magnetization. The degree of dominance of viscous magnetization is widely different for individual rock samples, but it can be classified into Type I, in which the viscous magnetization is much smaller than the stable one, and Type II which represents the viscous magnetization larger than the stable one. Most lunar igneous rocks belong to Type I, while the lunar fines and not impact-metamorphosed lunar breccias belong to Type II. It must be warned therefore that the viscous magnetic characteristics of individual lunar rock samples must be carefully examined, and thus the viscous magnetic component must be completely eliminated in every study of the lunar paleomagnetism.

It may be further advisable that a comparison of AF-demagnetization curve of NRM with that of artificially produced IRM of a nearly same intensity. Such a test give a semi-quantitative information of the stability of observed NRM of lunar rocks. Preferably, the thermal demagnetization test also may be requested in order to confirm a magnetically stable component of NRM of individual lunar rocks, though the thermal demagnetization procedure is generally a little too laborious.

An unusually strong magnetism is found from lunar igneous rock returned by Apollo 14 Mission. The particular sample, 14053, contains about 1 weight percent of metallic iron. However, it has not yet been clarified whether or not this sample can represent a certain general type of lunar igneous rocks in a certain locality on the Moon's surface. Another unsolved problem in the lunar rock magnetism may be concerned with the discovery of magnetite phase in some Apollo 12 lunar rocks (12030–23 and 12018–47) by Runcorn *et al.* (1971). Despite a considerable continuous effort to search such a magnetite phase in other lunar rocks, the authors have not yet

been able to find it. This problem may therefore be considered still pending in regard to the population of this magnetic phase in the lunar materials.

Acknowledgements

The authors' thanks are due M. D. Fuller and J. R. Dunn of University of Pittsburgh for their cooperation and assistance in the thermal demagnetization experiment. They are also indebted to M. Kono and Y. Aoki of University of Tokyo for their assistance during the whole course of measuring the magnetization versus temperature relationship. The authors also acknowledge the cooperation of S. V. Radcliffe of Case-Western Reserve University for allowing us to make measurements on NRM of samples, 12038–29, 12038–32, 14063–47 and 14310–159.

References

Bozorth, R. M.: 1951, *Ferromagnetism,* Van Nostrand, pp. 1–968.

Doell, R. R., Grommé,, C. S., Thorpe, A. N., and Senftle, F. E.: 1970, *Proc. Apollo 11 Lunar Sci. Conf.*, Vol. **3**, pp. 2097–2102.

Dyal, P., Parkin, C. W., Sonett, C. P., DuBois, R. L., and Simmons, G.: 1971, Apollo 14 Prelim. Sci. Rep., NASA SP-272, pp. 227–237.

Gaunt, P.: 1960, *Phil. Mag.* **8**, 1127–1148.

Grommé, C. S. and Doell, R. R.: 1971, *Proc. Second Lunar Sci. Conf.*, Vol. **3**, pp. 2491–2499.

Hargraves, R. B. and Dorety, N.: 1971, *Proc. Second Lunar Sci. Conf.*, Vol. **3**, pp. 2477–2483.

Helsley, C. E.: 1970, *Proc. Apollo 11 Lunar Sci. Conf.*, Vol. **3**, pp. 2213–2220.

Ishikawa, Y. and Akimoto, S.: 1958, *J. Phys. Soc. Japan* **13**, 1298–1310.

Larochelle, A. and Schwarz, E. J.: 1970, *Proc. Apollo 11 Lunar Sci. Conf.*, Vol. **3**, pp. 2305–2308.

Levinson, A. A. and Taylor, S. R.: 1971, *Moon Rocks and Minerals*, Pergamon Press, New York, pp. 1–222.

Mason, B. and Melson, W. G.: 1970, *The Lunar Rocks*, Wiley-Interscience, New York, pp. 1–129.

Nagata, T., Ishikawa, Y., Kinoshita, H., Kono, M., Syono, Y., and Fisher, R. M.: 1970, *Proc. Apollo 11 Lunar Sci. Conf. Geochim. Cosmochim. Acta Suppl. 1*, Vol. **3**, pp. 2325–2340.

Nagata, T., Fisher, R. M., Schwerer, F. C., Fuller, M. D., and Dunn, J. R.: 1971, *Proc. Second Lunar Sci. Conf.*, Vol. **3**, pp. 2461–2476.

Néel, L.: 1949, *Ann. Géophys.* **5**, 99–136.

Runcorn, S. K., Collinson, D. W., O'Reilly, W., Battey, M. H., Stephenson, A., Jones, J. M., Mauson, A. J., and Readman, P. W.: 1971, *Proc. Apollo 11 Lunar Sci. Conf.*, Vol. **3**, pp. 2364–2388.

Runcorn, S. K., Collinson, D. W., O'Reilly, W., Stephenson, A., Greenwood, N. N., and Battey, M. H.: 1971, *Second Lunar Science Conference* (Unpublished proceedings).

Sawaoka, A., Miyahara, S., and Akimoto, S.: 1968, *J. Phys. Soc. Japan* **25**, 1253–1257.

Shenoy, G. K., Kalvius, G. M., and Hafner, S. S.: 1969, *J. Appl. Phys.* **40**, 1314–1316.

Schwarz, E. J.: 1970, *Proc. Apollo 11 Lunar Sci. Conf.*, Vol. **3**, pp. 2389–2398.

Strangway, D. W., Larsen, E. E., and Pearce, G. W.: 1970, *Proc. Apollo 11 Lunar Sci. Conf.* Vol. **3**, pp. 2435–2452.

Swann, G. A., Bailey, N. G., Bastan, R. M., Eggelton, R. E., Hait, M. H., Holt, H. E., Larson, K. B., McEwen, M. C., Mitchell, E. D., Schaber, G. G., Schafer, G. P., Shepard, A. B., Sutton, R. L., Trask, N. J., Ulrich, G. E., Wilshire, H. G., and Wolfe, E. W.: 1971, 'Preliminary Geologic Investigations of the Apollo 14 Landing Site', Apollo 14 Prelim. Sci. Rep., NASA SP-272, pp. 39–85.

Wasilewski, P. J.: 1969, 'Correspondence Between Magnetic and Textural Changes in Titanomagnetites in Basaltic Rocks', D.Sc. Thesis, Univ. of Tokyo, Fac. Sci.

Wohlfarth, E. P.: 1963, 'Permanent Magnetic Materials', in *Magnetism*, Vol. **3** (ed. G. T. Rado and H. Suhl), Acad. Press, New York, pp. 351–393.